

# No evidence for the cold spot in the NVSS radio survey

Kendrick M. Smith<sup>1</sup> and Dragan Huterer<sup>2</sup>

<sup>1</sup> *Institute of Astronomy, Cambridge University, Madingley Road, Cambridge CB3 0HA, UK*

<sup>2</sup> *Department of Physics, University of Michigan, 450 Church St, Ann Arbor MI 48109, USA*

27 November 2018

## ABSTRACT

We revisit recent claims that there is a “cold spot” in both number counts and brightness of radio sources in the NVSS survey, with location coincident with the previously detected cold spot in WMAP. Such matching cold spots would be difficult if not impossible to explain in the standard  $\Lambda$ CDM cosmological model. Contrary to the claim, we find no significant evidence for the radio cold spot, after including systematic effects in NVSS, and carefully accounting for the effect of *a posteriori* choices when assessing statistical significance.

**Key words:** cosmology: cosmic microwave background, large-scale structure

## 1 INTRODUCTION

Cosmic microwave background (CMB) maps have been studied in detail during the last few years. These studies have been motivated by the remarkable full-sky high-resolution maps obtained by WMAP (Bennett et al. 2003; Spergel et al. 2007), and led to a variety of interesting and unexpected findings. Notably, various anomalies have been claimed pertaining to the alignment of largest modes in the CMB (de Oliveira-Costa et al. 2004; Hajian & Souradeep 2003; Slosar & Seljak 2004; Tegmark et al. 2003; Schwarz et al. 2004; Land & Magueijo 2005b,a; Copi et al. 2006), the missing power on large angular scales (Spergel et al. 2003; Copi et al. 2007), and the asymmetries in the distribution of power (Eriksen et al. 2004; Bernui et al. 2006; Hajian 2007). In the future, temperature maps obtained by the Planck experiment, and large-scale polarization information (Dvorkin et al. 2008) may be key to determining the nature of the large-scale anomalies. For a review of the anomalies and attempts to explain them, see Huterer (2006).

Recently, a paper by Rudnick et al. (2007) attracted particular attention, as it claimed to have detected a ‘cold spot’ — a drop in the source density *and* brightness in the NVSS survey. This claim would be relatively unremarkable, if it were not for the fact that a previously reported, anomalously cold spot in the WMAP microwave signal (Vielva et al. 2004; Cruz et al. 2005, 2006, 2007; Cayón et al. 2005) apparently lies at roughly the same location.

This claim, if verified to be true at high statistical significance, would represent a major result, and would be difficult or impossible to explain in the standard cosmological model. One interpretation, proposed in Inoue & Silk (2006) and Rudnick et al. (2007), is the existence of a large ( $\gtrsim 100$

Mpc) void at  $z \sim 1$ , which gives rise to an NVSS underdensity directly, and gives rise to the WMAP cold spot via the nonlinear ISW effect. However, the probability of forming such a large void in  $\Lambda$ CDM cosmology is negligibly small.

Here we reexamine these claims using our own analysis procedure, carefully including known systematic and statistical properties of NVSS (declination-dependent “striping” and galaxy-galaxy correlations; see §3.1), and marginalizing *a posteriori* choices when assessing statistical significance. We will argue that there is no statistically significant evidence for either a dip in NVSS number counts or median source flux in the WMAP cold spot. We will see that it is possible to construct statistics containing *a posteriori* choices (e.g., the location and radius of a “sub-disc” of the cold spot) which might appear to support an underdense region, but the statistical significance goes away when these choices are properly marginalized. Furthermore, we will show that by making different *a posteriori* choices, we could find evidence for an *overdense* region with the same statistical significance as an underdense region.

The paper is organized as follows. In §2 we describe the NVSS data and selection cuts that we consider. In §3 we perform statistical tests using the number density distribution of NVSS sources, and in §4 we do the same for the flux distribution. In §5 we study the dependence of our results on the selection cuts that are applied to the NVSS catalog prior to the analysis. Our main result, showing significance of anomalous number counts or source fluxes in the WMAP cold spot, using several different statistics and with a range of possible selection cuts in the NVSS catalog, is shown in Table 1. We conclude in §6.

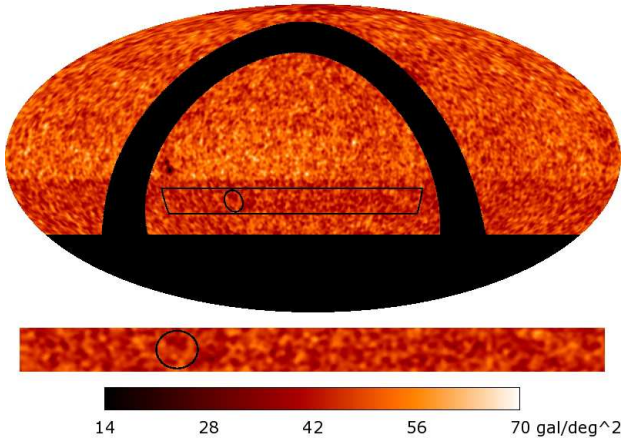


**Figure 1.** Galaxy count maps for the NVSS survey, smoothed to  $1^\circ$  radius and plotted in equatorial coordinates, with default data cuts as described in §2. The full sky counts (top panel) show declination-dependent variations in completeness level; the WMAP cold spot (shown as a circle in both panels) is entirely contained within the underdense “stripe” at declination  $\delta \lesssim -10^\circ$ . If we zoom in on a box at the same declination as the cold spot, then the WMAP cold spot does not look anomalous by eye (bottom panel; shown as a rectangular region in the top panel).

## 2 DATA

The NRAO VLA Sky survey (NVSS) is a 1.4 GHz continuum survey, covering 82% of the sky, with a source catalog containing over  $1.8 \times 10^6$  sources that is 50% complete at 2.5 mJy. Away from the galactic plane, almost all of the sources are extragalactic: quasars, or AGN-powered or star-forming galaxies. The NVSS catalog covers a wide range of redshifts (the median redshift is  $z \approx 0.9$ ), but dividing the catalog into redshift bins is not possible because per-source redshifts are not measured. However, in §5 we will explore the effect of dividing the catalog into flux bins.

When making Healpix (Gorski et al. 2005) maps from the NVSS catalog, we mask pixels near the galactic plane ( $|b| < 10^\circ$ ) or the boundary of the survey (declination  $\delta < -37^\circ$ ). Our “default cuts” will consist of this pixel mask, plus dropping all sources which are flagged in the NVSS catalog as having complex structure. (These are mainly galactic sources; if they are included in the maps then spurious features can be seen by eye at low galactic latitude.) We will also consider other choices of cuts in §5.

In Fig. 1, we show a full-sky map and a zoomed-in region near the WMAP cold spot, with default selection cuts and smoothed to  $1^\circ$  resolution. We have shown the full-sky map in equatorial coordinates to highlight a known systematic effect in NVSS (Blake & Wall 2002): the presence of declination-dependent variations in completeness level, most notably the underdense “stripe” at  $\delta \lesssim -10^\circ$ . Because the WMAP cold spot is inside the stripe, modeling these variations will play an important role in the analysis, as we will see in detail below.

## 3 GALAXY COUNT ANALYSIS

In Cruz et al. (2005), the WMAP cold spot is given as a circular region with center  $P_0$  at  $(l, b) = (209^\circ, -57^\circ)$  in galactic coordinates, and radius  $r_0 = 5^\circ$ . However, in Rudnick et al. (2007) the most anomalously underdense circular region in NVSS is quoted as having center  $P'_0$  at  $(l, b) = (207.03, -54.85)$  and radius  $r'_0 = 1^\circ$ . How does this mismatch between the WMAP cold spot and the NVSS underdense region affect the analysis?

The total statistical significance of the WMAP cold spot is only  $\approx 3\sigma$ . Presumably, at this significance, the best-fit center and radius have non-negligible statistical errors, and any nontrivial shape or substructure of the cold spot is not resolved.

For this reason, it seems reasonable to look for an NVSS underdensity ( $P'_0, r'_0$ ) which need not be equal to the WMAP cold spot ( $P_0, r_0$ ). However, this makes statistical significance more difficult to assess: for a correct treatment, the parameters ( $P'_0, r'_0$ ) must be treated as *a posteriori* choices. Alternately, one could simply ask whether the region ( $P_0, r_0$ ) is underdense in NVSS. In this case there are no *a posteriori* choices (we are simply counting NVSS galaxies using the best-fit cold spot parameters from WMAP data alone) and computing statistical significance is straightforward.

Our perspective is that either of these analyses is valid; in the next three subsections we consider the following possibilities for a disc-shaped NVSS underdensity with center  $P$  and radius  $r$ :

1.  $P = P_0, r = r_0$ : The NVSS underdensity has the same center and radius as the WMAP cold spot.
2.  $P = P_0, r \neq r_0$ : The NVSS underdensity has the same center as the WMAP cold spot but its radius is different; then we must assign statistical significance in a way which incorporates the *a posteriori* choice of radius.
3.  $P \subseteq P_0, r \neq r_0$ : The NVSS underdensity lies wholly within the WMAP cold spot but both its center and its radius are different; then we must incorporate the *a posteriori* choice of both radius and location.

### 3.1 Case 1: Fixed center, fixed radius

This case ( $P = P_0, r = r_0$ ) corresponds to the simplest possible question: if we count the total number of galaxies in the WMAP cold spot, do we get an anomalous value? We introduce the ratio statistic,

$$\frac{N_{\text{gal}}(P_0, r_0)}{\langle N_{\text{gal}}(P_0, r_0) \rangle} \quad (1)$$

and ask whether it differs from 1.0 with statistical significance, where the numerator  $N_{\text{gal}}(P_0, r_0)$  denotes the number of galaxies in the WMAP cold spot ( $P_0, r_0$ ) and the denominator is its expectation value.

Two issues arise here: first, how should the denominator  $\langle N_{\text{gal}}(P_0, r_0) \rangle$  be computed? The simplest prescription would be to assume that the expected number density per unit area is equal to the full-sky NVSS average:

$$\langle N_{\text{gal}}(P, r) \rangle = \pi r^2 \langle n \rangle_{\text{full-sky}} \quad (2)$$

where  $\langle n \rangle_{\text{full-sky}}$  is the mean number density per unit area on the full NVSS sky. This simple estimate for  $\langle N_{\text{gal}} \rangle$  is not satisfactory because it does not account for the underdense

stripe (see Fig. 1). Therefore, we also consider an improved prescription based on a simple stripe model. We assume that the expected number of galaxies in each Healpix pixel  $p$  is equal to the average taken over unmasked pixels  $p'$  at the same declination:

$$\langle N_{\text{gal}}(P, r) \rangle = \sum_{p \in (P, r)} \langle N_{\text{gal}}(p') \rangle_{p' \sim p} \quad (3)$$

where the sum runs over pixels  $p$  in the disc  $(P, r)$ , and  $\langle N_{\text{gal}}(p') \rangle_{p' \sim p}$  denotes the average galaxy count taken in pixels  $p'$  at the same declination as  $p$ .

The second issue when studying the ratio statistic in Eq. (1) is how error bars should be assigned. Here, the simplest prescription would be to assume Poisson statistics: we take the uncertainty in the numerator to be given by

$$\Delta N_{\text{gal}}(P, r) = \langle N_{\text{gal}}(P, r) \rangle^{1/2} \quad (4)$$

This simple prescription for  $(\Delta N_{\text{gal}})$  underestimates the error bars because it assumes that the NVSS galaxies are pure shot noise, i.e. galaxy-galaxy correlations are ignored.<sup>1</sup> Therefore, we also consider an improved prescription: we estimate  $(\Delta N_{\text{gal}})$  directly from the data by taking the RMS fluctuation over alternate choices  $P'$  of ring center which lie at the same declination as  $P$ :

$$\frac{\Delta N_{\text{gal}}(P, r)}{\langle N_{\text{gal}}(P, r) \rangle^{1/2}} = \text{RMS}_{P' \sim P} \left( \frac{N_{\text{gal}}(P', r) - \langle N_{\text{gal}}(P', r) \rangle}{\langle N_{\text{gal}}(P', r) \rangle^{1/2}} \right) \quad (5)$$

where the notation  $\text{RMS}_{P' \sim P}(\cdot)$  denotes the RMS fluctuation taken over choices of center  $P'$  with the same declination as  $P$ .<sup>2</sup>

With default cuts (§2), we find the following results. If we use full-sky averaging (Eq. (2)) and Poisson errors (Eq. (4)), then the WMAP cold spot appears to be underdense in NVSS sources at  $3.1\sigma$ . However this is simply an artifact of using the full-sky average galaxy density when computing  $\langle N_{\text{gal}} \rangle$ ; in fact, the WMAP cold spot is contained within the underdense NVSS stripe (Fig. 1). If we improve the estimate of  $\langle N_{\text{gal}} \rangle$  by using isolatitude averaging (Eq. (3)) then the cold spot appears *overdense* at  $1.1\sigma$ . This is already not statistically significant, but if we improve the estimate of  $\Delta N_{\text{gal}}(P, r)$  using Eq. (5), then the overdensity drops to  $0.8\sigma$ . We conclude that the WMAP cold spot, taken as a whole, is not underdense or overdense in NVSS sources, but modeling the NVSS “stripe” plays a crucial role in the analysis.

We note that declination-dependent striping is unlikely to affect the analysis of Rudnick et al. (2007), which is restricted to small regions of sky near the cold spot. The

<sup>1</sup> In principle, this could be remedied by estimating the galaxy power spectrum and including it in Monte Carlo simulations, although this may be difficult in practice, due to the presence of long-wavelength instrumental power in NVSS at low flux levels (Smith et al. 2007; Ho et al. 2008) which may not be accurately modeled by an isotropic Gaussian field. In Eq. (5), we have taken a simpler approach by averaging over choices of disc center  $P'$  in the real NVSS data, rather than averaging over Monte Carlo simulations.

<sup>2</sup> As a minor point, in Eq. (5) we have normalized each value of  $N_{\text{gal}}$  by its Poisson error  $\langle N_{\text{gal}} \rangle^{1/2}$  before taking the RMS; this slightly improves the estimate of  $(\Delta N_{\text{gal}})$  by accounting for variations in  $\langle N_{\text{gal}} \rangle$  due to striping and the pixel mask.

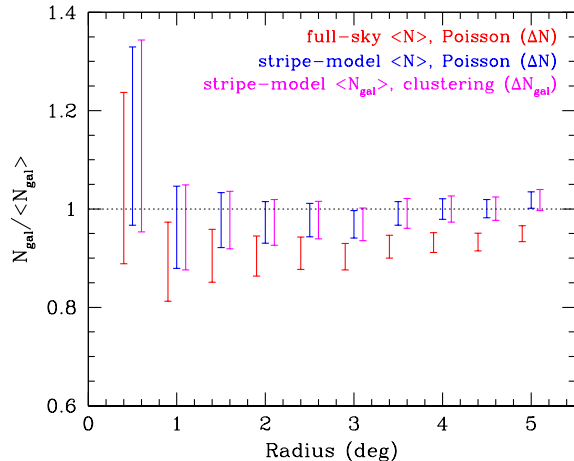


**Figure 2.** Galaxy counts in circles of varying radii centered at the WMAP cold spot location, relative to expected counts as in Eq. (1). From left to right, the three sets of error bars (all 68% C.L.) represent increasingly accurate analysis methods. The left errorbars assume full-sky  $\langle N_{\text{gal}} \rangle$  and Poisson  $(\Delta N_{\text{gal}})$  (Eqs. (2), (4)). The middle and right errorbars incorporate declination striping in  $\langle N_{\text{gal}} \rangle$  and galaxy-galaxy clustering in  $(\Delta N_{\text{gal}})$  respectively (Eqs. (3), (5)). It is seen that if the NVSS underdense stripe is not modeled, then the WMAP cold spot appears to be anomalously underdense, but the statistical significance is lost when the stripe is included in the analysis.

discussion here is intended to motivate expressions such  $(\Delta N_{\text{gal}})$  above (Eq. (3), and related quantities later in the paper, which are defined in a way which is robust to striping.

### 3.2 Case 2: Fixed center, floating radius

We next consider the possibility of an underdense region with the same center  $P = P_0$  as the WMAP cold spot but arbitrary radius  $r < r_0$ . We again define a ratio statistic

$$\frac{N_{\text{gal}}(P_0, r)}{\langle N_{\text{gal}}(P_0, r) \rangle} \quad (6)$$

and compute the expectation value  $\langle N_{\text{gal}}(P_0, r) \rangle$  and RMS deviation  $\Delta N_{\text{gal}}(P_0, r)$  following the discussion in the preceding subsection.

Results using this statistic are shown (with default cuts) in Fig. 2. The rightmost error bars represent our most accurate ways of computing  $\langle N_{\text{gal}} \rangle$  and  $(\Delta N_{\text{gal}})$  (Eqs. (3), (5)); we find that all points are within  $1\sigma$  of the expected level, i.e. no evidence for an underdensity is seen. (We note that if say, one value of  $r$  gave an anomalous value, then we would have to incorporate the *a posteriori* choice of  $r$  when assessing significance; we revisit this issue in §5.) The left and middle error bars represent less accurate ways of computing  $\langle N_{\text{gal}} \rangle$  and  $(\Delta N_{\text{gal}})$  (Eqs. (2), (4)) and are shown for comparison.

### 3.3 Case 3: Floating center, floating radius

The result of the preceding subsection appears to contradict Fig. 5 in Rudnick et al. (2007), where a statistically significant underdense disc of radius  $r'_0 = 1^\circ$  is seen. However, this figure has been constructed taking the disc center  $P'_0$  to be

the point  $(l, b) = (207.03, -54.85)$  rather than the center  $P_0$  of the WMAP cold spot which is at  $(l, b) = (209, -57)$ .

If the choice of  $(P'_0, r'_0)$  had an *a priori* motivation, then we would find, using an analysis similar to §3.1, a  $2.0\sigma$  underdensity, with our default cuts. (There are other underdense “subdiscs” as well, e.g. we find that the subdisc centered at  $(l, b) = (206.82, -56.4)$  with radius  $2.5^\circ$  is underdense at  $3.06\sigma$  if *a posteriori* choices are ignored.) However, we see no *a priori* motivation for making such choices of  $(P'_0, r'_0)$ , and we must therefore incorporate the effect of the *a posteriori* choice when calculating statistical significance.

To assess significance fairly, we incorporate the effect of the choice of  $(P'_0, r'_0)$  as follows. Formally, given a disc  $(P, r)$ , define the “naive number of sigmas” of its worst underdense subdisc by:

$$N_\sigma(P, r) = \min_{(P', r') \subset (P, r)} \left( \frac{N_{\text{gal}}(P', r') - \langle N_{\text{gal}}(P', r') \rangle}{\Delta N_{\text{gal}}(P', r')} \right) \quad (7)$$

where the notation  $\min_{(P', r') \subset (P, r)}(\cdot)$  means that the quantity in parentheses is minimized over discs  $(P', r')$  which are entirely contained in  $(P, r)$ , with minimum radius  $r'_{\text{min}} = 1^\circ$ . In this notation, the existence of the “subdisc”  $(P'_0, r'_0)$  from the preceding paragraph can be rephrased as the statement that  $N_\sigma(P_0, r_0) = -3.06$ , where  $(P_0, r_0)$  are the cold spot center and radius respectively.

To assess whether this value is anomalous, we evaluate the same statistic (“number of sigmas of the worst underdense subdisc”) in an ensemble of disc-shaped regions with the same size and declination as the WMAP cold spot. This way of assessing significance accounts for both the *a posteriori* choice of  $(P'_0, r'_0)$  and declination-dependent striping. More precisely, we compute  $N_\sigma(P, r_0)$  for an ensemble of alternate choices of disc center  $P$  with the same declination as the WMAP cold spot center  $P_0$ , and with radius  $r_0 = 5^\circ$ . We find that this ensemble of values has mean  $\langle N_\sigma \rangle = -2.65$  and RMS error  $(\Delta N_\sigma) = 0.45$ . Therefore, the cold spot (with  $N_\sigma = -3.06$ ) is typical among discs with the same radius and declination, and the “subdisc” described above does not have statistical significance after the effect of *a posteriori* choices is taken into account.

#### 4 FLUX ANALYSIS

In addition to number counts, the median NVSS brightness was also reported to be low near the WMAP cold spot in Rudnick et al. (2007). Since brightness is roughly proportional to (source counts)  $\times$  (source flux), and we have already analyzed the source counts, our perspective is that it is better to separate the two issues and next ask whether median source fluxes in NVSS are anomalous in the WMAP cold spot. Considering source counts and fluxes separately, rather than using brightness maps, has two additional advantages. First, it allows the analysis to proceed from the NVSS source catalog, thus avoiding instrumental complexities associated with working with the NVSS images, which have been incorporated by the NVSS team when constructing the source catalog. Second, it avoids introducing more *a posteriori* choices which must be marginalized (e.g. in Rudnick et al. (2007), the brightness maps are convolved with an 800 arcsec filter to obtain a continuous field, which is then median-filtered in sliding boxes with side length  $3.4^\circ$ ;

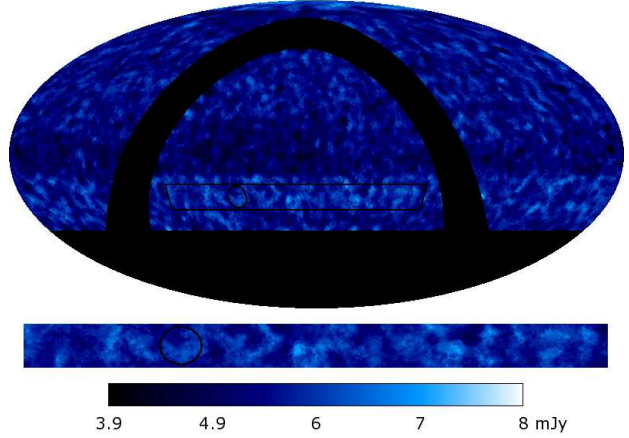


**Figure 3.** NVSS flux maps, smoothed by  $2^\circ$  median filtering as described in §4, shown with default cuts in equatorial coordinates. As in the galaxy count case (Fig. 1), the full-sky map (top panel) shows declination-dependent variations in median flux, and the WMAP cold spot (shown as a circle) is not anomalous by eye when viewed in a “box” at the same declination (bottom panel).

a “dip” is then observed at a point other than the WMAP cold spot center.)

We would also like to emphasize that, if the purpose of this analysis is to find voids, then there is no *a priori* motivation for considering either brightness or source fluxes; the best-motivated statistics would be based on number counts alone. Nevertheless, in this section, we will briefly NVSS source fluxes in the WMAP cold spot. Our median flux analysis will be analogous to the galaxy count case from the preceding section; we summarize our methodology and results here.

In Fig. 3, we show a flux map obtained by taking the median flux of all NVSS sources within  $2^\circ$  of each pixel. This median-based smoothing procedure was used because the NVSS flux distribution contains far outliers; if the mean were used instead of the median, then the map would be dominated by a small number of rare bright sources. Note that declination-dependent striping is seen in the flux map, as seen previously for number counts (Fig. 1).

Given disc center  $P$  and radius  $r$ , we define  $\mu(P, r)$  to be the median flux of all NVSS galaxies contained in the disc  $(P, r)$ , and consider ratio statistics of the form:

$$\frac{\mu(P, r)}{\langle \mu(P, r) \rangle} \quad (8)$$

We estimate the expected median flux  $\langle \mu(P, r) \rangle$  directly from the data by averaging over alternate choices of center  $P'$  with the same declination as  $P$ :

$$\langle \mu(P, r) \rangle = \langle \mu(P', r) \rangle_{P' \sim P} \quad (9)$$

We also estimate the error  $(\Delta \mu(P, r))$  from the data in an analogous way<sup>3</sup>

<sup>3</sup> Note that we have taken the factor  $\langle N_{\text{gal}} \rangle^{1/2}$  inside the RMS average, to improve the estimate of  $(\Delta \mu)$  by accounting for the scaling  $(\Delta \mu \propto N_{\text{gal}}^{-1/2})$  expected due to variations in number density alone.

$$\Delta\mu(P, r) = \frac{\text{RMS}_{P' \sim P} \langle N_{\text{gal}}(P', r) \rangle^{1/2} (\mu(P', r) - \langle \mu(P', r) \rangle)}{\langle N_{\text{gal}}(P, r) \rangle^{1/2}} \quad (10)$$

We then consider three cases for the disc  $(P, r)$ , as in §3.1–§3.3.

1. Fixed center, fixed radius ( $P = P_0, r = r_0$ ): In this case, we simply evaluate the ratio statistic in Eq. (8), taking  $(P, r)$  to be the WMAP cold spot center and radius  $(P_0, r_0)$ . We find that the ratio exceeds 1.0 by  $0.6\sigma$ , i.e. the median flux of all NVSS galaxies in the WMAP cold spot is not anomalous.

2. Fixed center, floating radius ( $P = P_0, r < r_0$ ): In this case, we compute the ratio statistic in Eq. (8) for a variety of radii centered at the cold spot center  $P_0$  (in analogy with Fig. 2). We find that all values are within  $1.2\sigma$  of 1.0, i.e. no anomalous value of the median flux is found.

3. Floating center, floating radius ( $P \subseteq P_0, r < r_0$ ): In this case, we choose a subdisc  $(P, r)$  of the WMAP cold spot  $(P_0, r_0)$  which appears to give the most anomalous value of the ratio statistic in Eq. (8). If we look for an anomalously low median flux, then we find that the subdisc with center  $(l, b) = (206.81, -54.75)$  and radius  $1^\circ$  appears to be low at  $2.2\sigma$ , if the *a posteriori* choice of  $(P, r)$  is temporarily ignored. To assess whether this value is really anomalous, we proceed in parallel with the number count analysis in §3.3: we evaluate the same statistic (naive “number of sigmas”  $N_\sigma$  of the most anomalous subdisc”) over an ensemble of regions with the same size and declination as the cold spot. We get  $N_\sigma = (2.2 \pm 0.3)$  in this ensemble, i.e. the WMAP cold spot (with  $N_\sigma = 2.2$ ) is a typical member of this ensemble, and the low flux in the aforementioned subdisc has no statistical significance.

## 5 ALTERNATE CHOICES OF CUTS

We have now performed an exhaustive analysis of NVSS number density (§3) and median flux (§4) in subspots of the WMAP cold spot, with three cases depending on whether the subspot location and radius are determined *a priori* or *a posteriori*, for a total of six analyses in all. This has been done using our “default cuts” from §2: we drop NVSS sources flagged as having complex structure to be conservative, but do not impose flux cuts, in order to avoid making an *a posteriori* choice of flux range.

One possible loophole remains: in Fig. 5 in Rudnick et al. (2007), the statistical significance appears to be much higher if only sources with flux  $S \geq 5$  mJy are retained. In this section, we consider the general question: can we get a statistically significant result if we use selection cuts other than our default choice?

We divide the NVSS catalog into four flux bins, with delimiting values given by  $\{3, 5, 12\}$  mJy. We also consider either dropping or retaining sources flagged as having complex structure in the NVSS catalog. For reference, the source density of NVSS is  $46 \text{ deg}^{-2}$  with complex sources dropped, or  $49 \text{ deg}^{-2}$  with complex sources retained. The delimiting values for our four flux bins were chosen to further divide the catalog into quartiles.

In Table 1, we summarize the results of repeating the six analyses considered in this paper with various sets of

cuts. This table presents many results in compressed form and is organized as we now explain.

Columns labeled “Fixed center, fixed radius” correspond to case 1 in §3–4: we simply compute the total number (or median flux) of galaxies inside the WMAP cold spot, and report the deviation (in “sigmas”) from the expected value. A positive sign indicates a result (either count or flux) which is larger than expected; a negative sign indicates a result which is less than the expected value.

Columns in Table 1 labelled “floating center, floating radius” correspond to case 3 in §3–4. Each entry in these columns corresponds to a complete analysis along the lines of §3.3 and has been calculated as follows.

We first compute the statistic  $N_\sigma(P_0, r_0)$ , defined in Eq. (7) to measure the “number of sigmas” of the worst underdense subdisc of the WMAP cold spot  $(P_0, r_0)$ . As explained in §3.3, this statistic cannot be used directly to assess significance since the subdisc is an *a posteriori* choice. We therefore define

$$\mathcal{N}_{\text{under}} = \frac{N_\sigma(P_0, r_0) - \langle N_\sigma \rangle}{\Delta N_\sigma} \quad (11)$$

where  $\langle N_\sigma \rangle$  and  $(\Delta N_\sigma)$  are the mean and RMS of the quantity  $N_\sigma(P_0, r_0)$  taken over an ensemble of regions with the same size and declination as the cold spot. For example, with default cuts, the analysis in §3.3 can be summarized by the statement that  $N_\sigma(P_0, r_0) = -3.06$  and  $\mathcal{N}_{\text{under}} = (-3.06 + 2.65)/0.45 = -0.9$ . The interpretation is that the “floating center, floating radius” analysis has found an underdense subdisc of the cold spot with significance  $0.9\sigma$ .

The sign convention in Eq. (11) has been chosen so that a negative value of  $\mathcal{N}_{\text{under}}$  corresponds to an underdensity which is more anomalous than the ensemble mean. A positive sign would mean that the most underdense subdisc in the WMAP cold spot is less anomalous than expected, when compared to an ensemble of regions with the same size and declination as the cold spot.

We define a quantity  $\mathcal{N}_{\text{over}}$  in an analogous way, choosing the sign so that a positive value corresponds to an overdense region which is more anomalous than the ensemble mean.

In Table 1, we report either  $\mathcal{N}_{\text{under}}$  (indicated by a negative sign) or  $\mathcal{N}_{\text{over}}$  (indicated by a positive sign), *whichever is more anomalous*. A ‘—’ entry means that  $\mathcal{N}_{\text{under}}$  is positive and  $\mathcal{N}_{\text{over}}$  is negative, i.e. we find no subdisc (either underdense or overdense) of the cold spot which is more anomalous than the ensemble mean, for a given set of cuts.

For example, with default cuts, we find a negative value for  $\mathcal{N}_{\text{over}}$ , i.e. the most anomalously overdense subdisc of the WMAP cold spot is actually less overdense than the ensemble mean. Therefore, the corresponding entry in Tab. 1 is given by  $\mathcal{N}_{\text{under}} = -0.9$ . This value summarizes the analysis from §3.3: with default cuts, we find a subdisc which is anomalously underdense at  $0.9\sigma$  (and any overdense subdisc is less anomalous than this).

Finally, columns in Table 1 labelled “fixed center, floating radius” correspond to case 2 from §3–4, with one difference: when reporting the significance of the most anomalous radius  $r$ , we incorporate the *a posteriori* choice of radius by maximizing over  $r$  as in case 3. (We omitted this step for

Flux range	NVSS galaxy counts analysis			NVSS median flux analysis		
	WMAP center and radius	WMAP center, any radius	Any center, any radius	WMAP center and radius	WMAP center, any radius	Any center, any radius
$S \leq 3$ mJy	$-0.5\sigma$ ( $-0.5\sigma$ )	$-0.8\sigma$ ( $-0.7\sigma$ )	— ( $-0.0\sigma$ )	$0.1\sigma$ ( $0.2\sigma$ )	$0.2\sigma$ ( $0.2\sigma$ )	— (—)
$3 \leq S \leq 5$ mJy	$0.4\sigma$ ( $0.2\sigma$ )	— (—)	— (—)	$1.1\sigma$ ( $0.9\sigma$ )	$0.3\sigma$ (—)	$2.5\sigma$ ( $-2.9\sigma$ )
$5 \leq S \leq 12$ mJy	$2.6\sigma$ ( $2.3\sigma$ )	$2.0\sigma$ ( $1.6\sigma$ )	$1.7\sigma$ ( $1.7\sigma$ )	$0.4\sigma$ ( $0.1\sigma$ )	$-0.9\sigma$ ( $-0.9\sigma$ )	$1.4\sigma$ ( $1.3\sigma$ )
$S \geq 12$ mJy	$-0.4\sigma$ ( $-0.6\sigma$ )	— ( $-0.2\sigma$ )	$-1.4\sigma$ ( $-1.6\sigma$ )	$1.3\sigma$ ( $0.5\sigma$ )	$-1.4\sigma$ ( $-1.2\sigma$ )	$-1.6\sigma$ ( $-2.2\sigma$ )
$S \leq 5$ mJy	$-0.2\sigma$ ( $-0.3\sigma$ )	$-0.5\sigma$ ( $-0.6\sigma$ )	— ( $-0.1\sigma$ )	$0.8\sigma$ ( $0.8\sigma$ )	$0.1\sigma$ ( $0.1\sigma$ )	$0.3\sigma$ ( $0.2\sigma$ )
$S \geq 5$ mJy	$1.4\sigma$ ( $1.0\sigma$ )	$0.6\sigma$ ( $-0.2\sigma$ )	$-1.8\sigma$ ( $-2.5\sigma$ )	$-1.7\sigma$ ( $-1.7\sigma$ )	$-1.1\sigma$ ( $-1.0\sigma$ )	$-1.6\sigma$ ( $-2.0\sigma$ )
Arbitrary $S$	$0.9\sigma$ ( $0.5\sigma$ )	$-0.1\sigma$ ( $-0.6\sigma$ )	$-0.9\sigma$ ( $-1.2\sigma$ )	$0.7\sigma$ ( $0.5\sigma$ )	$0.4\sigma$ ( $0.2\sigma$ )	$-0.6\sigma$ ( $-0.8\sigma$ )

**Table 1.** Statistical significance of anomalous NVSS number counts or median flux in the WMAP cold spot, for different NVSS flux ranges, and with complex sources either dropped (unparenthesized values) or retained (parenthesized) in the analysis. The six columns correspond to the different number count and median flux analyses that we have considered in §3–§4. As described in §5, each entry in the table is either the statistical significance of a region with high source density/flux (positive sign), or low source density/flux (negative sign), depending on which has higher significance. An entry is marked ‘—’ if we do not find any subdisc (either overdense or underdense) which is more anomalous than expected from statistics. (This is assessed by comparing to an ensemble of regions with the same size and declination as the cold spot, as explained in detail in §5.) As described in the text, the NVSS source density is roughly  $46 \text{ deg}^{-2}$ , the flux ranges chosen in the table roughly divide the catalog into quartiles, and the disks used in the analysis have radii in the range  $1 \leq r \leq 5$  deg. Thus the disks used to construct the table contain between  $\approx 36$  and  $\approx 3600$  sources.

simplicity in §3–4 because with our default cuts, all choices of  $r$  turned out to give very typical values.)

There are a few values in Table 1 which might be interpreted as statistically significant, e.g. the example which motivated this section: for the flux range  $S \geq 5$  mJy, there is a subdisc (the “floating center, floating radius” case) which has galaxy counts low at  $2.5\sigma$  even after accounting for the *a posteriori* choice of center and radius. However, we note that the statistical significance goes away when complex sources are dropped, or if we restrict the flux range further. Furthermore, one can find another value in the table which supports an *overdensity* with the same statistical significance (the “fixed center, fixed radius” galaxy count case with flux range  $5 \leq S \leq 12$  mJy). Given the large number of entries in Table 1, a few high-significance values such as these are expected as statistical events.<sup>4</sup>

Analogously, for the flux analysis, there is a  $2.9\sigma$  low-flux subdisc in the flux range  $3 \leq S \leq 5$  mJy, but if complex sources are dropped, we find a  $2.5\sigma$  *high-flux* disc in the same flux range. Since there is no clear pattern to the few high-significance values, and since a high source density/flux region is supported as well as a low source/flux region, our interpretation of Table 1 is that there is no evidence for either NVSS number counts or median source fluxes which are atypical in the WMAP cold spot.

## 6 DISCUSSION AND CONCLUSIONS

In this paper, we have revisited claims from Rudnick et al. (2007) that there is a cold spot in the NVSS radio survey which is statistically significant and aligned with the cold

<sup>4</sup> To make this more quantitative, given only 4 independent events, the likelihood that one event is anomalous at the  $2.5\sigma$  level is  $\approx 2\sigma$ , so getting a few such anomalous values in an analysis such as Table 1 with many different choices of cuts is not surprising.

spot found in WMAP (Vielva et al. 2004; Cruz et al. 2005). We found no evidence for either an underdensity in NVSS number counts, or a region of atypical median source flux.

Our analysis incorporates systematic declination-dependent striping in NVSS, by estimating quantities such as  $\langle N_{\text{gal}}(P, r) \rangle$  directly from the data via isolatitude averaging (e.g. Eq. (3)). In an analogous way, we incorporate statistical clustering of galaxies in NVSS by estimating variances over isolatitude rings (e.g. Eq. (5)).

Simple, direct statistical tests, such as counting the total number of all NVSS galaxies in the WMAP cold spot, or taking the median flux of all such galaxies, do not show any statistically significant anomaly. (This corresponds to case 1 in §3–4.) Things only become murky when one considers statistics with many *a posteriori* choices, such as an anomalous subdisc of the cold spot (case 3), or a choice of selection cuts which maximizes the quoted significance (Table 1). We have exhaustively studied many such statistical tests and argued that when the *a posteriori* choices are included in the assessment of statistical significance, there is no evidence for an NVSS “cold spot”.

As a concrete example, consider the “ $S \geq 5$  mJy” case in Fig. 5 of Rudnick et al. (2007), which seems to show a  $\approx 5\sigma$  underdense region, if the errorbars are taken at face value. We agree with the number counts that are plotted in this figure, but disagree that there is statistically significant evidence for an underdensity. Let us illustrate this by following this example through the steps of this paper one at a time. First, if we use our most accurate prescriptions for the RMS error ( $\Delta N_{\text{gal}}$ ) and the expected count ( $\langle N_{\text{gal}} \rangle$ ) (Eqs. (3), (5)), then we find that the statistical significance drops to  $3.4\sigma$ ; however this ignores the effect of *a posteriori* choices. The center of this underdense region is not the WMAP cold spot center, and if we account for this choice (and the *a posteriori* choice of radius) using the method of §3.3, then we find that the significance decreases to  $2.5\sigma$ .

This now accounts for the *a posteriori* choice of subdisc, and appears to give a statistically significant result, but

we have still made an *a posteriori* choice of selection cuts, by allowing complex structure and considering only sources with flux  $S \geq 5$  mJy. When viewed in the larger context of Table 1, it is seen that these choices maximize the quoted “number of sigmas” of an underdensity, and simply reflect the large number of possible choices of selection cuts: the significance goes away if the cuts are changed slightly, and in fact a different choice of cuts would favor an *overdensity* rather than an underdensity, with roughly the same significance. This last observation is perhaps the most convincing sign that the apparent  $\approx 2.5\sigma$  underdensity, for a single choice of selection cuts, is spurious.

For the median flux analysis (§4), our conclusions are the same: we find no evidence for atypical source fluxes in the WMAP cold spot, after accounting for *a posteriori* choices. There are a few choices of cuts which appear to show anomalous values (if the *a posteriori* choice of cuts is ignored), but the number of such values is consistent with statistics, and the cuts can be tuned to support either a region with high or low source density/flux with roughly the same statistical significance (Table 1).

We do not see reason to give preferential treatment to *a posteriori* choices in the analysis and selection cuts given in Rudnick et al. (2007), and we instead considered a range of analyzed quantities and selection criteria. Had there been a physical reason or a survey-specific requirement for the particular treatment of raw data used in Rudnick et al. (2007), we would have agreed with that choice being well motivated or even necessary. However, since we do not see such motivation, we insist on calling all such choices *a posteriori*.

In McEwen et al. (2007), the cold spot was identified as one of 18 regions which are “peaks” in the ISW cross-correlation between WMAP and NVSS. However, this analysis was performed using wavelet smoothing with scale  $250'$  and would be blind to the  $1^\circ$  underdense region studied in Rudnick et al. (2007). Furthermore it is not clear from the analysis in McEwen et al. (2007) whether the WMAP-NVSS cross-correlation is statistically significant when restricted to the cold spot alone.

Despite the null result of this paper, one should not be disheartened. More detailed observation of the cold spot region in galaxy surveys will likely improve confidence about the existence of any over/underdensity or lack thereof. More generally, new WMAP data and the eagerly expected Planck maps expected in a few years, combined with data from a variety of galaxy surveys from ground and space, will provide a gold mine to search for signatures of the early and late-universe physics in the large-scale structure and the CMB.

## ACKNOWLEDGMENTS

We would like to thank Lawrence Rudnick, Cora Dvorkin, Eiichiro Komatsu, Wayne Hu, and David Spergel for useful discussions. KMS was supported by an STFC Postdoctoral Fellowship. DH was supported by the DOE OJI grant under contract DE-FG02-95ER40899, and NSF under contract AST-0807564.

## REFERENCES

- Bennett C. L., et al., 2003, ApJS, 148, 1  
 Bernui A., Vilella T., Wuensche C. A., Leonardi R., Ferreira I., 2006, Astron. Astrophys., 454, 409  
 Blake C., Wall J., 2002, Mon. Not. Roy. Astron. Soc., 329, L37  
 Cayón L., Jin J., Treaster A., 2005, MNRAS, 362, 826  
 Copi C. J., Huterer D., Schwarz D. J., Starkman G. D., 2006, Mon. Not. Roy. Astron. Soc., 367, 79  
 Copi C. J., Huterer D., Schwarz D. J., Starkman G. D., 2007, Phys. Rev. D, 75, 023507  
 Cruz M., Cayon L., Martinez-Gonzalez E., Vielva P., Jin J., 2007, Astrophys. J., 655, 11  
 Cruz M., Martinez-Gonzalez E., Vielva P., Cayón L., 2005, MNRAS, 356, 29  
 Cruz M., Tucci M., Martinez-Gonzalez E., Vielva P., 2006, Mon. Not. Roy. Astron. Soc., 369, 57  
 de Oliveira-Costa A., Tegmark M., Zaldarriaga M., Hamilton A., 2004, Phys. Rev., D69, 063516  
 Dvorkin C., Peiris H. V., Hu W., 2008, Phys. Rev., D77, 063008  
 Eriksen H. K., Hansen F. K., Banday A. J., Górski K. M., Lilje P. B., 2004, ApJ, 605, 14  
 Gorski K. M., et al., 2005, Astrophys. J., 622, 759  
 Hajian A., 2007, arXiv:astro-ph/0702723  
 Hajian A., Souradeep T., 2003, ApJ, 597, L5  
 Ho S., Hirata C. M., Padmanabhan N., Seljak U., Bahcall N., 2008, arXiv:0801.0642  
 Huterer D., 2006, New Astron. Rev., 50, 868  
 Inoue K. T., Silk J., 2006, Astrophys. J., 648, 23  
 Land K., Magueijo J., 2005a, Phys. Rev. Lett., 95, 071301  
 Land K., Magueijo J., 2005b, MNRAS, 357, 994  
 McEwen J. D., Vielva P., Hobson M. P., Martinez-Gonzalez E., Lasenby A. N., 2007, Mon. Not. Roy. Astron. Soc., 373, 1211  
 Rudnick L., Brown S., Williams L. R., 2007, ApJ, 671, 40  
 Schwarz D. J., Starkman G. D., Huterer D., Copi C. J., 2004, Phys. Rev. Lett., 93, 221301  
 Slosar A., Seljak U., 2004, Phys. Rev., D70, 083002  
 Smith K. M., Zahn O., Doré O., 2007, Phys. Rev., D76, 043510  
 Spergel D., et al., 2007, Astrophys. J. Suppl. 170  
 Spergel D. N., et al., 2003, ApJS, 148, 175  
 Tegmark M., de Oliveira-Costa A., Hamilton A. J., 2003, Phys. Rev., D68, 123523  
 Vielva P., Martinez-Gonzalez E., Barreiro R. B., Sanz J. L., Cayón L., 2004, ApJ, 609, 22